

Available online at www.sciencedirect.com**ScienceDirect**

Procedia - Social and Behavioral Sciences 96 (2013) 2692 – 2697

Procedia
Social and Behavioral Sciences

13th COTA International Conference of Transportation Professionals (CICTP 2013)

Novel Image Mosaic Algorithm for Concrete Pavement Surface Image Reconstruction

Hua Wang^{a*}, Xin Liu^a, Shen Zhang^a, Wei Quan^a^a*School of Transportation Science and Engineering, Harbin Institute of Technology, No.73 Huanghe Rd. NanGang Dist, Harbin,15001,China*

Abstract

In this paper, a novel image mosaic method for concrete pavement surface image sequences reconstruction has been proposed. Harris corner points are extracted uniformly from the overlapped areas of concrete pavement surface images, which are considered feature points. The commonly used circular projection method is applied for coarse matching step and an improved point matching method is proposed for invariance of image rotation and distortion. The image fusion strategy of fading in and fading out is employed for the smooth and seamless of mosaic image. For the practical pavement surface images, which exists rotation and distortion, the corresponding experimental results show that the proposed image matching method has higher precision and stronger robustness.

© 2013 The Authors. Published by Elsevier Ltd. Open access under [CC BY-NC-ND license](http://creativecommons.org/licenses/by-nc-nd/3.0/).

Selection and peer-review under responsibility of Chinese Overseas Transportation Association (COTA).

Keywords: concrete pavement surface; image fusion; image mosaic

1. Introduction

For the purpose of pavement automatic surveys, the high-resolution image sequence of pavement lanes whose entire width is 3.75 m is captured by the use of two or three cameras instead of a wide-view angle camera with limited resolution (Wang & Elliott, 1999; Hou, Wang, Wang, and Wang, 2007). In most cases, the overlapping areas in image sequence always cause some issues in counting the number of pavement cracks and lead to incorrect evaluation of pavement performance. In order to track the pavement surface condition more accurately and intelligently, the robust image mosaic algorithm, which is relatively independent of image rotation and distortion, is extremely desirable. In previous related works, many researchers focused on image registration algorithms which are also the key to deciding the output performance of image mosaicing algorithms. At present, many image registration algorithms have been proposed and an extensive and comprehensive survey is found in

* Corresponding author. Tel.: +86-451-86283036; fax: +86-451-86283779.

E-mail address: wanghua@hit.edu.cn

the literature (Brown, 1992; Zitova & Flusser, 2003). Sang & Zhang present a point pattern relaxation matching method, which is called Songnongs' algorithm and is invariant to rotation and scale changes (1998). In this paper, a robust and high-quality image mosaic algorithm is presented that takes the characteristic property of a concrete pavement surface into account.

2. Theories of Image Mosaic Processing

2.1. Image Preprocessing

The goal of image preprocessing is to improve the quality of source gray-level images. Image formation in the camera occurs from light reflected from the surrounding world. Due to the disturbance of both uneven brightness and the optical device of cameras, non-uniform gray intensity problems cannot be avoided (Sun, 2008). The expression for pavement surface image signals I is (Wang, 2004):

$$I = I_p + I_b + I_n \quad (1)$$

where I_p is the undisturbed image of the pavement surface, I_b is the uneven brightness and is a low frequency signals, and I_n is white Gaussian noise that is generated due to signal sampling and quantization. The unsharp masking algorithm (Deng, 2011) is used to remove uneven illumination I_b and the median filter is applied to suppress noise I_n .

2.2. Uniform Extraction of Harris Corner

The harris corner detector proposed by Harris and Stephens is based on the second moment matrix to extract corner features (1988). This approach is broadly used in detecting interest points due to its simple calculation and robustness. Harris corners of pavement surface images tend to appear nearby the cracks or irregular objects. Therefore, the pavement surface image is divided into sub-blocks to extract corners uniformly by applying the sub-blocks strategy proposed in the literature (Zhang, Liu, Pang, and Li, 2003).

2.3. Coarse Circular Projection Matching Algorithm

Image registration is the essential part of panoramic image creation. The definition given by Zitova & Flusser (2003) is "Image registration is the process of overlaying two or more images of the same scene taken at different times, from different viewpoints, and/or by different sensors. It geometrically aligns two images-the reference and sensed images." In this paper, the circular projection matching algorithm (Xu, Wang, and Li, 2005) is employed to obtain the candidate matched point pairs.

2.4. Point Optimization Matching Algorithms

There are two most commonly method used for point optimization matching. One is the traditional point pattern relaxation matching algorithm, which basic concepts and operations are introduced as follows (Ranade & Rosenfeld, 1980), the other is the four-element relaxation matching algorithm, which is proposed by Sang and Zhang (1998).

2.5. Improved Four-element pattern Relaxation Matching Algorithm

An improved four-element relaxation matching algorithm based on known candidate matched point pairs is proposed when larger random walk errors exist between two point sets. The approach also has the anti-rotation

and anti-scale advantages of Sangnong’s algorithm and shows a higher tolerance for random walk errors. The whole algorithm flow is as follows:

Step 1: The angle difference θ between Set Q and Set P is defined as:

$$\Delta p_1 = p_h - p_i \tag{2}$$

$$\Delta p_2 = p_u - p_i \tag{3}$$

$$\Delta q_1 = q_h - q_i \tag{4}$$

$$\Delta q_2 = q_u - q_i \tag{5}$$

The scalar angle $|\theta_1|$ of vector Δp_2 and vector Δp_1 and scalar angle $|\theta_2|$ of vector Δq_2 and vector Δq_1 are calculated using equation 6 and equation 7, respectively as:

$$|\theta_1| = \arccos\left(\frac{\Delta p_1 \cdot \Delta p_2}{\|\Delta p_1\| \cdot \|\Delta p_2\|}\right) \tag{6}$$

$$|\theta_2| = \arccos\left(\frac{\Delta q_1 \cdot \Delta q_2}{\|\Delta q_1\| \cdot \|\Delta q_2\|}\right) \tag{7}$$

Therefore, the angle difference θ is

$$\theta = \begin{cases} |\theta_1| - |\theta_2| & (\Delta p_1 \times \Delta p_2) \text{ and } (\Delta q_1 \times \Delta q_2) \text{ are in the same direction} \\ |\theta_1| + |\theta_2| & (\Delta p_1 \times \Delta p_2) \text{ and } (\Delta q_1 \times \Delta q_2) \text{ are in opposite direction} \end{cases} \tag{8}$$

Step 2: Let $\phi^{iihh}(u, u)$ be the support function of the four-element point set (p_i, q_i, p_h, q_h) given by point pair (p_u, q_u) . The support function is based on variable θ , such that

$$\phi^{iihh}(u, u) = \frac{1}{f(\theta)} \tag{9}$$

Where $f(\theta)$ is the support core function with respect to random walk errors. The following equation is designed to enhance the tolerance for random walk errors:

$$f(\theta) = \begin{cases} a^{\theta/\theta_r} & \theta < \theta_r \\ e^{\theta/\theta_r} & \theta_r \leq \theta \leq \theta_m \\ \infty & \theta > \theta_m \end{cases} \tag{10}$$

where a is the base number of exponential function a^x . The angle θ_r is the lower limit of the tolerance for random walk errors and θ_m is the upper limit of the tolerance for random walk errors, which is the maximum value of angle θ . When $f(\theta) = 1$, θ_1 equals θ_2 and the displacement distance of q_u relative to q_i and q_j is equivalent to the distance of p_u relative to p_i and p_j . Therefore, point pair (p_u, q_u) gives the largest support to the four-element point set (p_i, q_i, p_h, q_h) .

Step 3: The largest support of the four-element point set (p_i, q_i, p_h, q_h) given by the rest of the point pairs can be described as:

$$\max_{u \neq i, u \neq h} \phi^{iihh}(u, u) \tag{11}$$

When the largest support of a four-element point set that consists of (p_u, q_u) and any other matched point pair is small, (p_u, q_u) is considered an incorrect matched point pair and is removed from Set Q and Set P .

2.6. Image Fusion

After image registration processing, Image T and Image S are transformed to the same rectangle coordinate system as the space transformation matrix M . The gray intensity at the coordinate (i, j) generally need to be interpolated with the neighboring transformed points to avoid an empty pixel from occurring (Li & Guo, 2007). The image fusion technique stitches two images together to create a seamless panorama image. Fading in and fading out is the most simple and direct solution in existing fusion methods. The fusion region $f_w(x, y)$ is given by:

$$f_w(x, y) = w \cdot f_{11}(x, y) + (1 - w) \cdot f_{22}(x, y) \quad (12)$$

where w is the change factor that gradually varies from 1 to 0, $f_{11}(x, y)$ and $f_{22}(x, y)$ define the overlapping of image T and S , respectively; and Δw is the step size given by:

$$\Delta w = 1 / L \quad (13)$$

where L is the column width of the overlapping region.

3. Experiments and results

One hundred concrete pavement surface images, which are captured from Ha-Tong Road in Heilongjiang province of China, are chosen to prove the effectiveness of the presented algorithm. The image mosaic experiments are run on Matlab 7.0.

Six randomly selected adjacent pavement surface image samples are shown in Figure 1 (a) to (f) for building a full-scene pavement surface image. Figures 2 (a) to (c) demonstrate that there are no obvious synthetic traces existing in the mosaicing image results caused by the algorithm proposed in this paper.

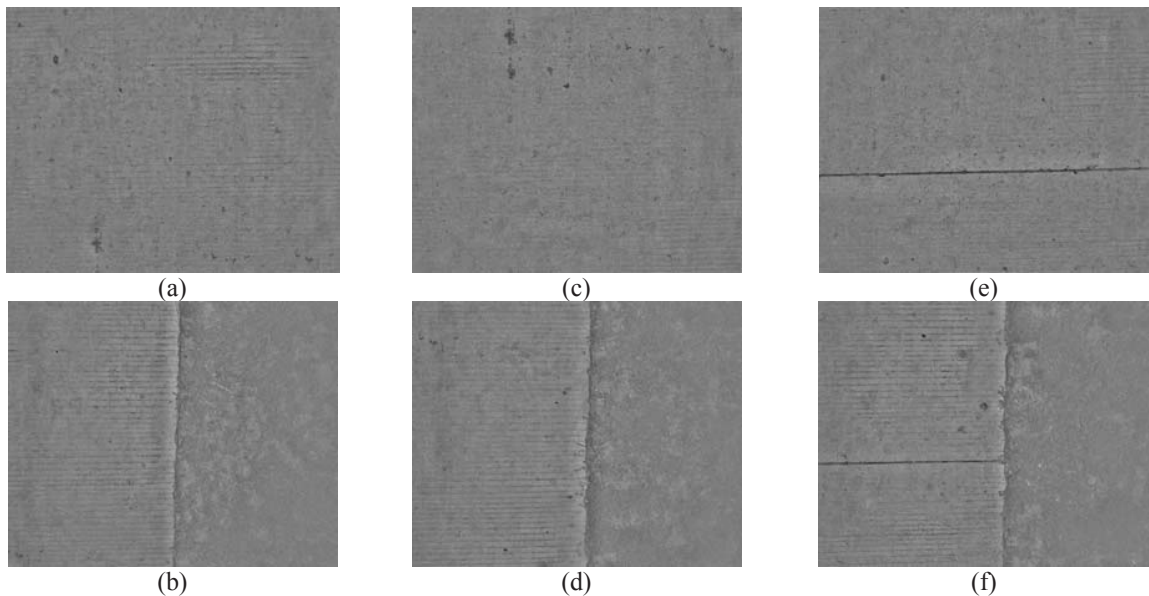


Fig.1. The adjacent image samples for stitching: (a) The reference image of group 1; (b) The sensed image of group 1; (c) The reference image of group 2; (d) The sensed image of group 2; (e) The reference image of group 3; (f) The sensed image of group 3

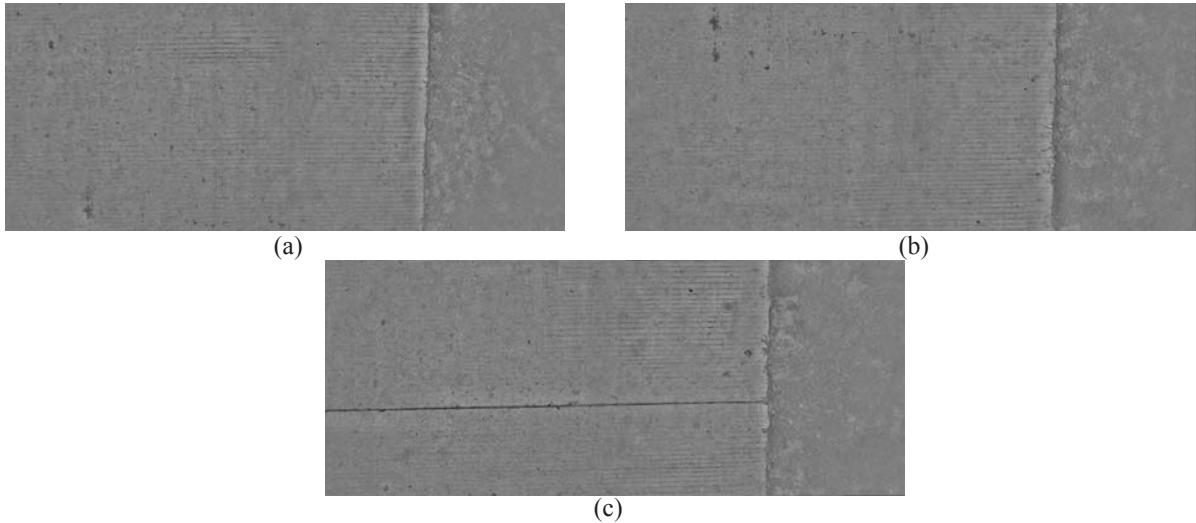


Fig.2. (a) The mosaicing result of group 1; (b) The mosaicing result of group 2; (c) The mosaicing result of group 3

Figure 2 (a), Figure 2 (b) and Figure 2 (c) are three transverse image mosaicing results. Generally, compared to Figure 10, there are random walk errors in Figure 2. That is, the transverse panorama images suffer more severe distortion. Figure 3 (a) is the mosaicing image result with Figure 2 (b) and (c) formed by using the proposed algorithm, Figure 3 (b) is the mosaicing image result with Figure 2 (a) and (b). Figure 3 (c) is the mosaicing image result with Figure 2 (b) and (c) formed by using Sangnong's algorithm instead of our optimization matching algorithm. As shown in Fig 3 (b), the performance of Sangnong's algorithm can't fulfill the mosaicing requirement of longitudinal pavement surface images under the same experimental conditions.

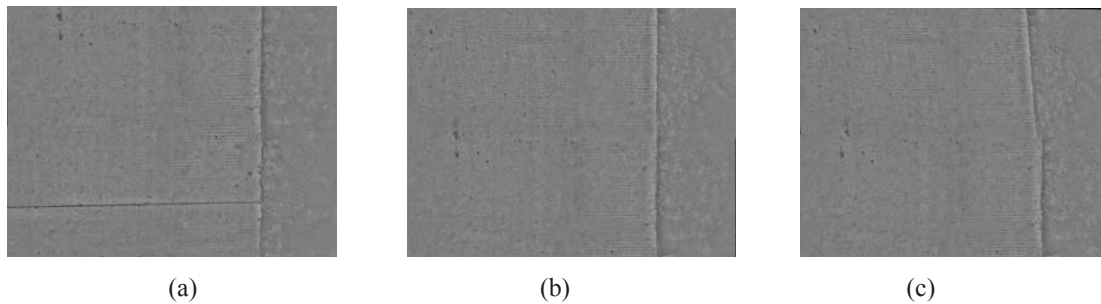


Fig. 3. (a) the mosaicing result of Figure 2 (b) and (c) using the proposed algorithm; (b) the mosaicing result of Figure 2 (a) and (b) using the proposed algorithm; (c) the mosaicing result of Figure 2 (a) and (b) using Sangnong's algorithm

4. Conclusion

In the case of larger random walk errors or distortions existing in images, the support of any point pair given by the rest of the correct point pairs or incorrect point pairs shows no deference with respect to Sangnong's algorithm or the traditional algorithm. This is the main reason that Sangnong's algorithm does not work well in the pavement surface image mosaicing experiments. The improved relaxation matching algorithm adjusts the

decreasing speed of the support in the point optimization process when the random walk errors have known limits. This enhances the robustness of the system to larger distortions.

Acknowledgements

This research was supported by the China National Science Foundation Grant No. 51138003 and Grant No. 61102038, and the Natural Science Foundation of Heilongjiang Province Grant No. QC2011C097.

References

- Brown, L. G. (1992). A survey of image registration techniques. *ACM computing surveys (CSUR)*, 24, 325-376.
- Deng, G. (2011). A generalized unsharp masking algorithm. *IEEE Transactions on Image Processing*, 20, 1249-1261.
- Harris, C., & Stephens, M. (1988). A combined corner and edge detector. In *Alvey vision conference (Vol. 15, pp. 50)*: Manchester, UK.
- Hou, X., Wang, H., Wang, Q., & Wang, Z. (2007). Development of automated inspection system for highway surface distress. In *Fundamental Problems of Optoelectronics and Microelectronics III* (pp. 65951Y-65951Y-65954): International Society for Optics and Photonics.
- Li, X., & Guo, B. (2007). An image mosaic method based on orientation feature of interest point. *Computer Engineering and Application*, 43, 26-28.
- Sang, N., & Zhang, T. (1998). Point pattern relaxation matching: invariant to rotations and scale changes. *Acta Electronica Sinica*, 6, 74-81.
- Ranade, S., & Rosenfeld, A. (1980). Point pattern matching by relaxation. *Pattern recognition*, 12, 269-275.
- Sun, Z. (2008). Reduce Non-uniform illumination achieved by Matlab. *Microcomputer Information*, 12, 313-314.
- Wang, H. (2004). A study on detection of pavement cracks based on fractal theory. Harbin Institute of Technology, Harbin.
- Wang, K. C., & Elliott, R. P. (1999). Investigation of image archiving for pavement surface distress survey. Mack-Blackwell Transportation Center, University of Arkansas, Fayetteville.
- Xu, Y., Wang, J., & Li, P. (2005). Research on scene matching method using circular projection. *Systems Engineering and Electronics*, 27, 1725-1728.
- Zhang, Q., Liu, Z., Pang, Y., & Li, W. (2003). Automatic registration of aerophotos based on SUSAN operator. *Acta Geodaetica et Cartographica Sinica*, 32, 245-250.
- Zitova, B., & Flusser, J. (2003). Image registration methods: a survey. *Image and vision computing*, 21, 977-1000.